JOURNAL OF NEUROTRAUMA 30:227–235 (February 1, 2013)

DOI: 10.1089/neu.2012.2504

Hindlimb Muscle Morphology and Function in a New Atrophy Model Combining Spinal Cord Injury and Cast Immobilization

Fan Ye,[1,*] Celine Baligand,[2,*] Jonathon E. Keener,[3] Ravneet Vohra,[1] Wootaek Lim,[1] Arjun Ruhella,[1] Prodip Bose,[3–5] Michael Daniels,[6] Glenn, A. Walter,[2] Floyd Thompson,[3,4,7] and Krista Vandenborne[1]

Abstract

Contusion spinal cord injury (SCI) animal models are used to study loss of muscle function and mass. However, parallels to the human condition typically have been confounded by spontaneous recovery observed within the first few post-injury weeks, partly because of free cage activity. We implemented a new rat model combining SCI with cast immobilization (IMM) to more closely reproduce the unloading conditions experienced by SCI patients. Magnetic resonance imaging was used to monitor hindlimb muscles' cross-sectional area (CSA) after SCI, IMM alone, SCI combined with IMM (SCI + IMM), and in controls (CTR) over a period of 21 days. Soleus muscle tetanic force was measured *in situ* on day 21, and hindlimb muscles were harvested for histology. IMM alone produced a decrease in triceps surae CSA to 63.9 ± 4.9% of baseline values within 14 days. In SCI, CSA decreased to 75.0 ± 10.5% after 7 days, and recovered to 77.9 ± 10.7% by day 21. SCI + IMM showed the greatest amount of atrophy (56.9 ± 9.9% on day 21). In all groups, muscle mass and soleus tetanic force decreased in parallel, such that specific force was maintained. Extensor digitorum longus (EDL) and soleus fiber size decreased in all groups, particularly in SCI + IMM. We observed a significant degree of asymmetry in muscle CSA in SCI but not IMM. This effect increased between day 7 and 21 in SCI, but also in SCI + IMM, suggesting a minor dependence on muscle activity. SCI + IMM offers a clinically relevant model of SCI to investigate the mechanistic basis for skeletal muscle adaptations after SCI and develop therapeutic approaches.

Key words: atrophy; immobilization; magnetic resonance imaging; SCI; skeletal muscle

Introduction

Skeletal muscle experiences extensive detrimental alterations after spinal cord injury (SCI), including profound atrophy and loss of muscle strength.[1] Impairments in skeletal muscle greatly increase the risk for secondary health complications, such as type 2 diabetes,[2] cardiovascular disease,[3,4] osteoporosis,[5] and fractures.[6] Strength of the lower extremity muscles has also proven to be an important predictor of locomotor recovery in persons with SCI.[7,8] Accordingly, the development of effective therapeutic strategies that promote the recovery of muscle mass and function after SCI is critically important.

Animal models of SCI have proven to be invaluable for the development of novel experimental therapies. Current animal models of SCI include complete transection, hemisection, compression, and contusion.[9–11] Models in which the spinal cord is sharply transected have been widely used to study the anatomic regeneration of axons, because they allow for a reproducible complete SCI. However, most human SCIs do not involve transection of the cord, and are caused by transient compression or contusion of the spinal cord.[12] Experimental contusion models of SCI have been developed that more closely reproduce important features of the pathology observed in clinical injuries.[11,13,14] These models have been widely used to characterize neuromuscular, pathophysiological, and functional changes after SCI.[14–17] and to assess the efficacy of rehabilitation strategies such as locomotor training.[18–24] Our group demonstrated that daily locomotor training in a moderate contusion SCI rat model accelerates muscle mass and force recovery.[20] However, the untrained animals also showed a progressive increase in muscle mass, suggestive of a considerable amount of spontaneous recovery. This recovery is likely the result of limb movement and loading (self-training) in the unrestricted

Departments of [1]Physical Therapy, [2]Physiology and Functional Genomic, [3]Physiological Sciences, [5]Neurology, and [7]Neuroscience, University of Florida, Gainesville, Florida.
[4]North Florida/ South Georgia Veterans Heath System, Brain Rehabilitation Research Center of Excellence, Gainesville, Florida.
[6]Section of Integrative Biology, University of Texas, Austin, Texas.
*The first two authors contributed equally.

setting of their home cage. Accordingly, the recovery induced by self-training in rodents can represent a limitation in the interpretation of pre-clinical rehabilitation studies and the transferability of findings in this model to patients.[18,19]

In a recent study, Caudle et al.[18] implemented wheelchair restriction in rats, starting 4 days after moderate contusion SCI, to limit the amount of muscle afferent input during recovery. Even though unloading was periodic in this approach (up to 18 hours per day, 5 days per week), it demonstrated the considerable impact of free cage ambulation on functional recovery in contusion SCI animals. In order to reproduce the around-the-clock disuse condition experienced by patients more closely, we introduce a new rat model with SCI, which minimizes loading of the hindlimbs using cast immobilization. Cast immobilization models have long been used to study muscle adaptations during disuse in rodents,[25–27] and allow continuous restriction of activity and loading. The implementation of a modified rodent cast design model, allowing for bladder expression and appropriate animal care in contusion SCI animals, may offer a more clinically relevant approach to study therapeutic strategies targeting skeletal muscle in SCI.

The primary purpose of the present study was to develop and validate a new contusion SCI rat model, which minimizes loading of the hindlimbs by using cast immobilization. We compared this new model to two other models of disuse: cast immobilization alone and severe SCI alone. Using magnetic resonance imaging (MRI) we performed a noninvasive longitudinal assessment of changes in muscle size. In addition, *in situ* force mechanics and muscle histology were performed to further evaluate the effect of each of the models on muscle function and fiber morphology.

Methods

Animals

Adult female Sprague–Dawley rats (16 weeks, weighing 294 ± 16 g at the start of the study) were obtained from Charles River Laboratories and housed in a temperature (22 ± 1°C) and humidity ($50 \pm 10\%$) controlled room with a 12:12 h light:dark cycle. Animals were provided rodent chow and water *ad libitum* and were given 1 week to acclimatize to the environment. Fifty-six rats were randomly separated into four groups: severe SCI (SCI, $n = 19$), bilateral cast immobilization (IMM, $n = 12$) for 2 weeks, severe SCI plus 2 weeks of bilateral cast immobilization (SCI + IMM, $n = 12$) and control (CTR, $n = 12$). The timeline of the study is presented in detail in Figure 1. All procedures were performed in accordance with the United States Government Principle for the Utilization and Care of Vertebrate Animals and were approved by the Institutional Animal Care & Use Committee at the University of Florida. Experimental animals were given access to a soft high-protein content transgenic dough (Bio-Serv,NJ, product #S3472, 21.2% protein, 3.83 kcal/g), placed on the bottom of the cage.

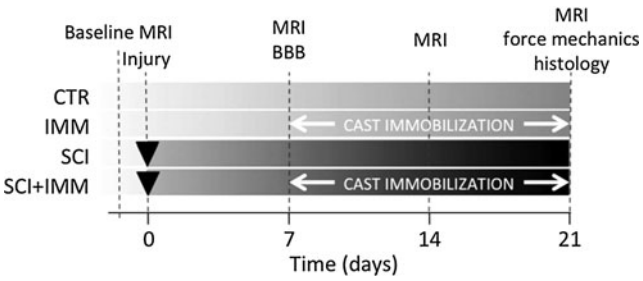

FIG. 1. Experimental time line of interventions and measurements in the four different groups. Black triangle indicates the day of spinal cord injury (SCI).

SCI procedure

All surgical procedures were performed under aseptic conditions. Severe SCI was produced using a NYU-MASCIS injury device as previously described.[14] Briefly, the animals were deeply anesthetized with a combination of ketamine (90 mg/kg body weight) and xylazine (8 mg/kg body weight) and a dorsal laminectomy was performed at the thoracic vertebral level T7-T9 to expose the spinal cord.[28] Clamps attached to the spinous processes of T7 and T9 stabilized the vertebral column. Contusion was produced by dropping a 10 g cylinder from the height of 50 mm onto the T8/T9 segment of the spinal cord. To further ensure the reproducibility of the injuries, the MASCIS device was connected to a computer to record force/velocity data from each drop (height: 50.52 ± 0.57 mm, velocity: -0.97 ± 0.01 m/sec, compression: 2.55 ± 0.44 mm). The impactor was left on the spinal cord for 7 sec after the drop. Analgesia was given in the form of Buprinex (0.025 mg/kg) and ketoprofen (22 mg/kg) once daily over the first 48 h after SCI. Subcutaneous lactated Ringers' solution and ampicillin (200 mg/kg) were administrated after completion of the surgery. The animals were kept under vigilant postoperative care, including daily examination for signs of distress, weight loss, dehydration, and bladder dysfunction. Manual expression of bladders was performed two to three times daily, as required, and animals were monitored for the possibility of urinary tract infection. Animals were housed individually. At postoperative day 7, open field locomotion was assessed during 4 min by two different scorers using the Basso, Beattie, Bresnahan (BBB) scoring scale[13] and two animals that did not fall within a preset score range (0–4) were excluded from the study and replaced by additional animals. A total of 49 surgical procedures were performed to account for potential attrition of the groups caused by possible surgical complication. Mortality rates are reported in the Results section.

Bilateral cast immobilization procedures

At day 8 after SCI, bilateral cast immobilization was performed on the rats assigned to the SCI + IMM and IMM groups. Briefly, rats were anesthetized with gaseous isoflurane (3% for induction, 0.5–2.5% for maintenance). The casting tape (Patterson Medical, Bolingbrook, IL) was applied on both hindlimbs using the following procedure. Joints were fixed at the following angles: ankle, 125 degrees, knee 180 degrees, and hip 160 degrees, except for a slight abduction. The casting tape encompassed the caudal fourth of the body (superior to tail); however, care was taken not to cover the abdominal region, to allow easy access for bladder expression in SCI + IMM. A thin layer of padding was placed underneath the casting tape in order to prevent skin abrasions. Slight pressure was applied when wrapping the casting tape on the body, so that there was minimal room for movement.

Daily preventive maintenance consisted of adjusting and replacing chewed-off casting tape. In addition, the rats were checked twice a day for skin lesions, hygiene, and fecal clearance. Animals maintained good mobility, healthy skin, normal grooming behaviors, and adequate food intake.

MRI

MR images of each of the hindlimbs were acquired separately at baseline and on days 7, 14, and 21, respectively, to noninvasively assess changes in muscle cross-sectional area (CSA) (Fig. 1). Experiments were performed in horizontal magnets at 4.7T using VnmrJ (Agilent, Inc., Palo Alto, CA) and at 11.1T using Paravision 3.0.2 (Bruker, Ettlingen, Germany). Animals were anesthetized with isoflurane (3% for induction, 1–2% for maintenance) and placed in a prone position on a plastic cradle. One foot was firmly secured with tape on a 5 mm thick support placed underneath the animal to ensure that the hindlimb was kept horizontal, centered and aligned with the z-axis of the magnet. For casted animals, the

foot support was 1 cm thick to match the cast thickness, and the animal body slightly angled for appropriate alignment of the hindlimb. A concave ^{1}H quadrature surface coil (2 cm × 4 cm) was placed on top of the lower hindlimb, centered on the belly of the muscle. Three-dimensional gradient echo images were acquired at 4.7T (TR/TE = 100/7.6 ms) or 11.1T (TR/TE = 120/5.4 ms) with a spatial resolution of $97 \times 97 \times 384\ \mu m^3$.

Images were converted to Digital Imaging and Communications in Medicine (DICOM) format using either Paravision for Bruker data, or a custom-made IDL code for Varian data (IDL, ITT Visual Information Systems, Boulder, CO), and analyzed with Osirix (www.osirix-viewer.com). Hypointense signal arising from the muscle facia provided sufficient contrast to allow for the delineation of the triceps surae (TS) muscle group (soleus and gastrocnemius) and the tibialis anterior (TA), as illustrated in Figure 2A. The maximal CSA (CSA_{max}) was calculated as the mean of the consecutive three greatest CSAs. CSA_{max} measurements on day 21 were compared with muscle wet weight (see next section) for methodological validation. To study the potential asymmetry in longitudinal changes of muscle size, an asymmetry index was defined as a relative difference between left and right hindlimb sizes (CSA_{left}-CSA_{right})/ average (CSA_{left},CSA_{right}) × 100.

Muscle force measurements and tissue harvest

At the end of the 3 week experiment, *in situ* soleus force measurements were performed on both hindlimbs as described previously.[29] Briefly, the rats were anesthetized with isoflurane (3% for induction, 1–2% for maintenance), and a small dorsal, midline incision was made to expose the gastrocnemius-soleus complex. The soleus and gastrocnemius muscles were carefully separated and the distal tendon of the soleus was connected to a variable range force transducer (Biopac Systems, Goleta, CA TSD105A) using a steel wire suture. The tibial nerve was surrounded by a bipolar electrode cuff proximal to its innervation to the soleus muscle. The animal was then placed in supine position, such that the soleus muscle was oriented in a horizontal plane, and the hindlimb was secured in placed by a pair of screw-driven pins at the condyles of the femur. The body temperature was maintained at 37°C, and a mineral oil drip (30°C) was used to maintain muscle temperature and prevent the muscle from drying during testing.

The soleus muscle was first stimulated using supramaximal (~7V, 0.2 msec) unidirectional square-wave pulses applied to the tibial nerve (Grass S88 stimulator; West Warwick, RI). The physiological tests were performed on the soleus adjusted to the isometric optimum length, determined by measuring maximal isometric forces generated at graded muscle lengths. Subsequently, three maximal isometric tetanic force measurements were performed with a 5 min interval between stimulations (20–30 V, 80 Hz, 1500 msec duration). The absolute peak tetanic force (P_0 in N) was recorded and normalized to muscle weight (MW in $N.g^{-1}$). Immediately after completion of the force mechanics the hindlimb muscles (soleus, gastrocnemius, TA, and extensor digitorum longus [EDL]) were harvested and weighed. The muscles were pinned at optimal length with optimal cutting temperature (OCT) compound, rapidly frozen in isopentane pre-cooled in liquid nitrogen, and subsequently stored at −80°C.

Immunohistochemistry

Immunohistochemistry was used to determine experimental changes in soleus and EDL muscle fiber size. Transversal cryostat sections (10 μm) were taken from the midbelly region and mounted serially on gelatin-coated glass slides. Rabbit anti-laminin (Neomarker, Labvision, Fremont, CA) and rhodamine-conjugated goat anti-rabbit IgG (Nordic Immunological Laboratories, Langendijk, The Netherlands) were used to outline the muscle fibers. Stained sections were mounted in mounting medium for fluorescence (Vector Laboratories, Burlingame, CA). Image acquisition and analysis was performed on a Leitz DMR microscope (Leica Camera Inc, Allendale, NJ). The average muscle fiber size (EDL and soleus) was determined in both legs of each animal based on analysis of 250–300 fibers at the mid-belly section, and the mean value and standard deviation of all animals is reported for each experimental group. The characteristics of the fiber size distribution were also examined. The full width at half maximum (FWHM) was used as an estimate of the extent or width of each distribution and to establish a discriminative threshold among the different groups.

Statistical analysis

Statistical analyses were performed on final sample sizes of $n = 12$ for CTR, IMM, and SCI + IMM, and $n = 19$ for SCI. All data

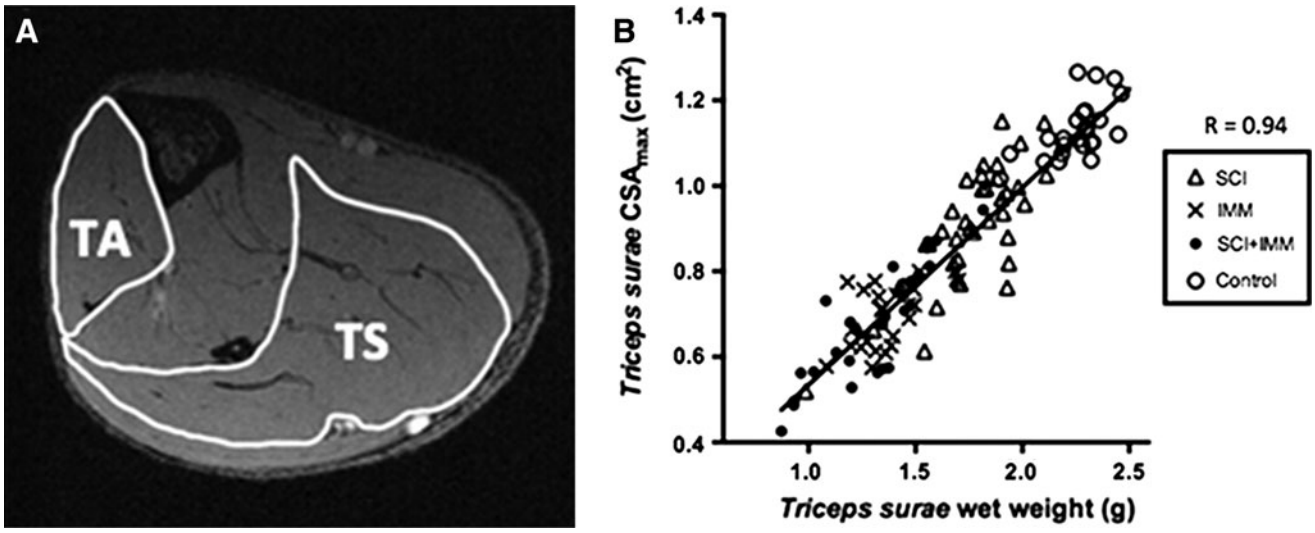

FIG. 2. (A) Example of MRI transverse image of the rat hindlimb. The tibialis anterior (TA) and triceps surae (TS) muscles are outlined in white. Data were acquired with a slice thickness of 385 μm and a field of view of $2.5 \times 2.5\ cm^2$. **(B)** Correlation between wet weight and CSA_{max} measured in the TS muscle in all groups on experimental day 21.

were analyzed using a mixed model with random subject effect, varying residual variance, and estimation of auto correlation parameters for repeated measurements. A Tukey's adjusted mean separation test was used to estimate which model-estimated least squares means were significantly different.

All data are presented as the simple means ± SD, unless specified differently in the text. Statistical significance was accepted for $p < 0.05$.

Results

Body weight and animal health

SCI + IMM animals showed normal grooming behaviors throughout the study and minimal skin abrasions. The animals were able to ambulate using their forelimbs, and maintained adequate food intake. We did not observe any sign of stress after cast immobilization. Body weight for each of the animal groups at the end of the 3 week experiment is provided in Table 1. Whereas baseline animal body weights were similar among groups, the body weights at 3 weeks of the CTR, SCI, IMM and SCI + IMM animals were 309 ± 18 g, 292 ± 18 g, 267 ± 10 g, and 281 ± 17 g, respectively (Table 1). The weight of the SCI + IMM animals was on average 10% lower than that of the control group, and not different in comparison with SCI. We observed a mortality rate of 18% 1 week after surgery. By the end of the 3 week experimental period, additional attritions of 14% and 25% were observed in the SCI and SCI + IMM groups, respectively. The mortality rate over the 3 week observation period was 29.5% in SCI and 38.5% in SCI + IMM.

Muscle wet weight

Muscle wet weight measurements acquired at the 3 week time point showed significant atrophy in all three experimental groups studied, compared with controls (Table 1). As expected, both SCI and IMM alone produced a marked loss in soleus absolute muscle weight (115 ± 20 g and 86 ± 8 g, respectively) compared with the control group (158 ± 17g, $p < 0.0001$). After normalization to body weight measured on day 21, the relative soleus muscle mass was decreased by 20% in the SCI group and by 25% in the IMM group compared with controls ($p < 0.05$). An additional 20% relative weight loss was observed in the soleus muscle of SCI + IMM animals compared with SCI animals ($p < 0.05$). The combination of SCI and bilateral cast immobilization also induced a greater relative muscle mass loss compared with SCI in the other muscles studied: TS, TA, and EDL (Table 1).

Muscle cross-sectional area

MRI was implemented to quantify *in vivo* longitudinal changes in muscle size in the three experimental groups. As an internal validation of our MRI measures, the relationship between CSA_{max} obtained on day 21 and wet weight of the TS, (sum of gastrocnemius and soleus), was examined. A strong correlation (Pearson coefficient of 0.94) was found between the two measures (Fig. 2B), which demonstrates that the *in vivo* MRI CSA measures reliably reflect measures of muscle mass in the posterior compartment.

The initial baseline CSA_{max} of the TS muscle group was 113.0 ± 7 mm^2. Figure 3 graphically illustrates the evolution of the average TS CSA_{max} in each of the groups relative to baseline values. The control group presented a non-significant relative increase in TS CSA_{max} within the course of the experiment (+3.3 ± 3.8 % on day 21, $p = 0.76$). On postoperative day 7, the TS CSA_{max} of SCI animals significantly decreased to 75.1 ± 10.5% of baseline values ($p < 0.0001$). In animals with SCI only, the CSA_{max} remained relatively stable over time and was 77.9 ± 10.7% of pre-injury levels by day 21 post-surgery. In the cast immobilization only (IMM) group, TS CSA_{max} decreased to 79.2 ± 5.4% on day 14 ($p < 0.0001$), after 1 week of immobilization, and showed a further decline in the second week, reaching 63.9 ± 4.9 % on day 21 ($p < 0.0001$). The largest amount of atrophy was observed in the SCI + IMM model (Fig. 3A), in which the TS CSA_{max} was decreased to 56.9 ± 9.9 % of baseline by day 21 ($p < 0.0001$).

The TA muscle CSA_{max} are presented in Figure 3B. IMM alone did not show a significant decrease in TA CSA_{max}. On the other hand, SCI alone induced a significant decrease in TA CSA_{max} on postoperative day 7 (79.4 ± 6.8%, $p < 0.0001$). A significant recovery was observed by postoperative day 21 ($p < 0.001$). This was prevented in the SCI + IMM group, in which atrophy was maintained throughout the experimental period.

Muscle force measurements

The peak tetanic force (P_0) measured in soleus muscles showed a significant decrease, compared with controls, in all the experimental conditions tested ($p = 0.0001$). At the 3 week time point, absolute peak P_0 was decreased by 25% in the SCI group, 42% in

Table 1. Muscle Wet Weight and Muscle Wet Weight/Body Weight for Hindlimb Muscles on Day 21. Data Are Presented as Mean ± SD

	CTR (n = *12*)	*IMM* (n = *12*)	*SCI* (n = *19*)	*SCI + IMM* (n = *12*)
Muscle wet weight (mg)				
Soleus	158 ± 17	86 ± 8*	115 ± 20*	81 ± 12*#
Triceps Surae	2244 ± 138	1364 ± 149*	1755 ± 224*	1295 ± 239*#
Tibilalis anterior	630 ± 41	528 ± 44*	527 ± 78*	452 ± 74*#
Extensor digitorum longus	155 ± 12	124 ± 8*	138 ± 16*	113 ± 15*#
Muscle wet weight/body weight on day 21 ($mg.g^{-1}$)				
Soleus	0.51 ± 0.05	0.32 ± 0.04*	0.40 ± 0.07*	0.29 ± 0.05*#
Triceps Surae	7.28 ± 0.45	5.11 ± 0.55*	6.01 ± 0.71*	4.62 ± 0.86*#
Tibilalis anterior	2.04 ± 0.08	1.98 ± 0.18	1.81 ± 0.26*	1.58 ± 0.27*#
Extensor digitorum longus	0.50 ± 0.03	0.47 ± 0.03*	0.46 ± 0.05*	0.39 ± 0.06*#
Body weight on day 21 (g)	309 ± 18	267 ± 10*	292 ± 18	281 ± 17*

*Significantly different from control.
#Significantly different from SCI ($p < 0.05$).

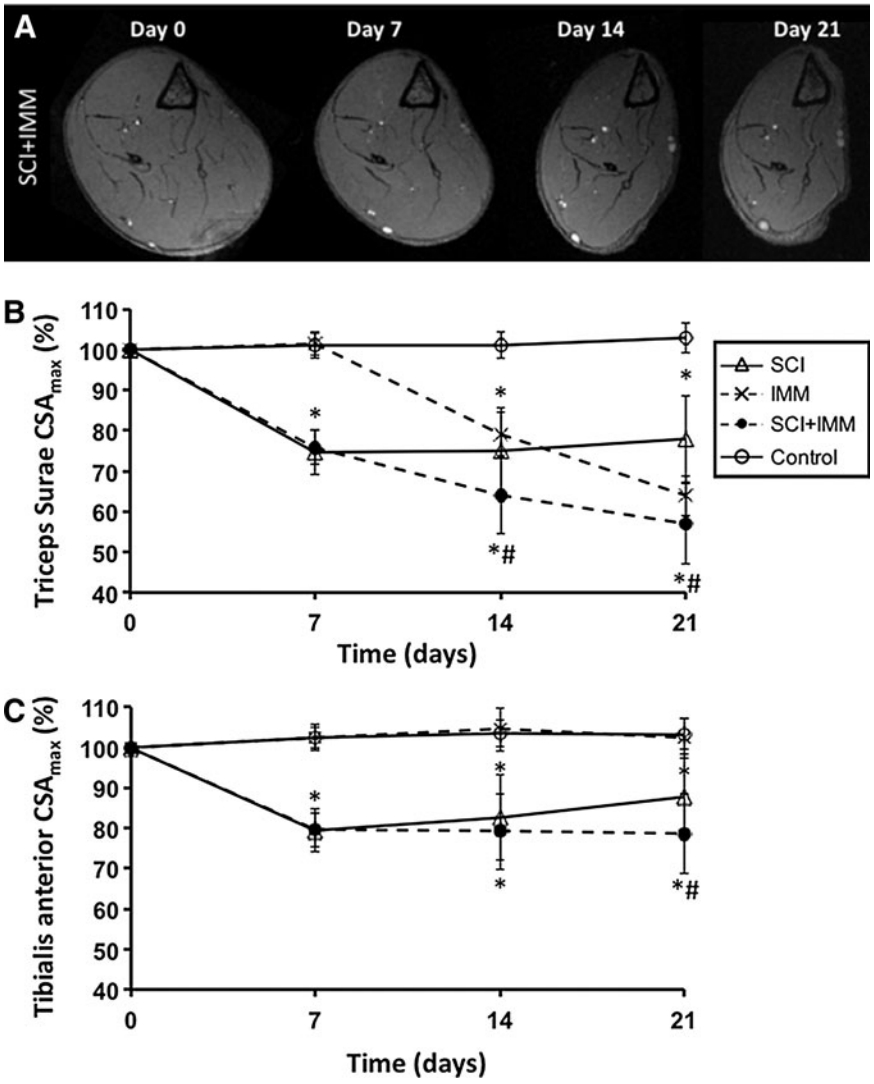

FIG. 3. Time course of the relative changes in triceps surae (TS) CSA_{max} in controls (CTR) spinal cord injured (SCI), immobilized (IMM), and both spinal cord injured and immobilized (SCI + IMM). **(A)** Example of transverse image of the hindlimb in a SCI + IMM rat on experimental days 0, 7, 14, and 21. **(B)** TS CSA_{max} and **(C)** tibialis anterior (TA) CSA_{max}, expressed as a percentage of baseline measurements as a function of time in all groups. *Significantly different from CTR. #Significantly different from SCI ($p < 0.05$)

the IMM group, and 46% in the SCI + IMM group compared with controls. The addition of the cast in the SCI + IMM group led to a significant additional loss of 22% compared with SCI alone ($p = 0.0001$). However, the normalized peak tetanic force for soleus muscles (normalized to muscle wet mass) did not significantly differ among the groups ($p = 0.85$) (Fig. 4).

Muscle fiber size

In the soleus muscle, SCI alone and IMM alone resulted in a 50% decrease in average muscle fiber size compared with controls (Fig. 5, $p < 0.05$). The decrease was more dramatic in the SCI + IMM group, with the soleus fibers being on average 66% smaller than in controls ($p < 0.05$). In the EDL muscle, a larger amount of atrophy was also observed in SCI + IMM compared with SCI alone ($p < 0.05$).

Frequency distributions of the soleus fiber size are displayed for each experimental condition in Figure 6. In control animals, fiber sizes were broadly distributed, ranging from 500 μm^2 to 6000 μm^2 approximately, which can be described by an FWHM of 2400 μm^2. In all experimental groups, fiber size distribution showed a leftward shift at the terminal time point, resulting in a large decrease in the FWHM (600 μm^2 in SCI and in SCI + IMM, 800 μm^2 in IMM), and a positive skewness of the histogram. Interestingly, the SCI + IMM showed the largest shift toward small size fibers. Only 5 % of the muscle fibers were < 1000 μm^2 in CTR animals, a threshold defined as the fifth percentile of the distribution. In contrast, 26% of soleus fiber sizes were below this threshold in CTR animals, 42% in IMM and up to 71 % in SCI + IMM.

Asymmetry in muscle size

The degree of asymmetry in muscle size between left and right hindlimbs for each group of animals was assessed and compared over time. At baseline, the asymmetry coefficient for the TS CSA_{max} ranged from 2.6 to 3.4% in all groups (Table 2). The cast immobilization procedure induced a rather symmetrical amount of atrophy, as shown by the 4.4 ± 1.2% coefficient of asymmetry on

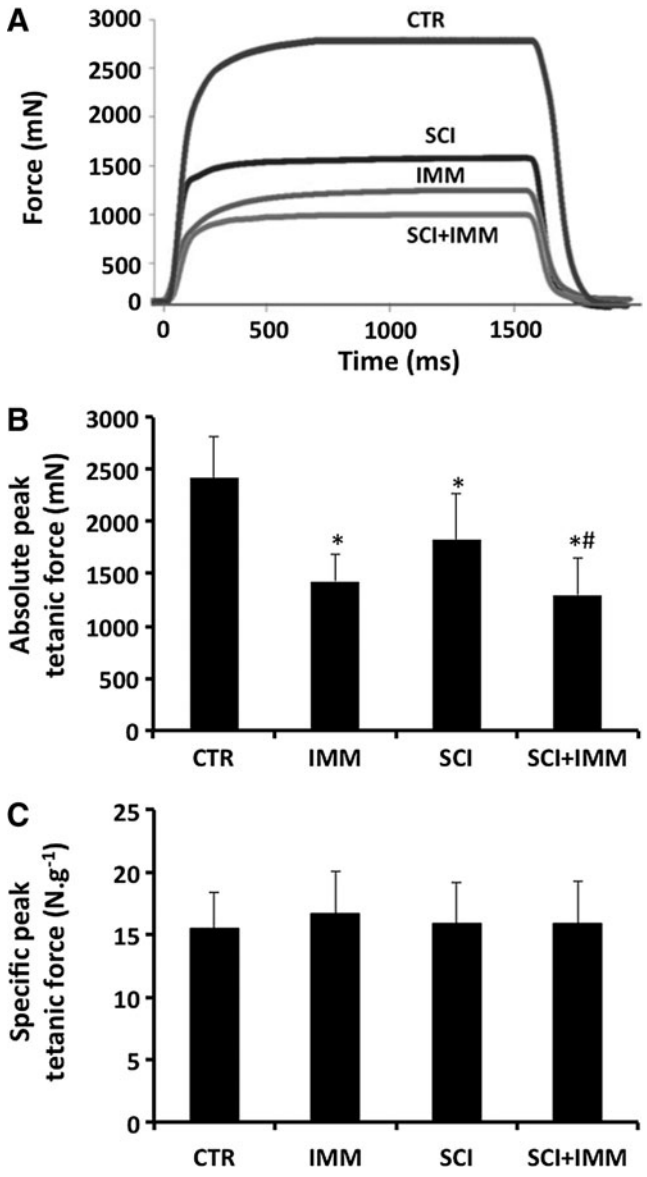

FIG. 4. *In situ* contractile properties of soleus muscle in the different models. **(A)** Representative experimental records of the force trace from the *soleus* muscle in controls (CTR) spinal cord injured (SCI), immobilized (IMM), and both spinal cord injured and immobilized (SCI + IMM). **(B)** Soleus absolute peak tetanic force (P_0), **(C)** Soleus specific peak tetanic force (P_0/MW). *Significantly different from CTR. #*Significantly* different from SCI ($p < 0.05$).

postoperative days 14 and 21, which was not significantly different from baseline levels of asymmetry ($p = 0.16$). Interestingly, whereas 1 week after SCI animals displayed a limited amount of asymmetry (6.9 ± 1.0 in SCI and 4.7 ± 0.8 in SCI + IMM), this progressively increased (Table 2). The asymmetry coefficient was 11.8 ± 2.4 on day 14 ($p = 0.002$) and 9.6 ± 2.4 on day 21 (Table 2). This elevation in the degree of muscle size asymmetry was not observed to be reduced by cast immobilization in the SCI + IMM group, and progressively reached significantly higher values at days 14 and 21 compared with day 7: 11.7 ± 2.3 on day 14, and 14.9 ± 3.4 on day 21, $p = 0.009$, respectively.

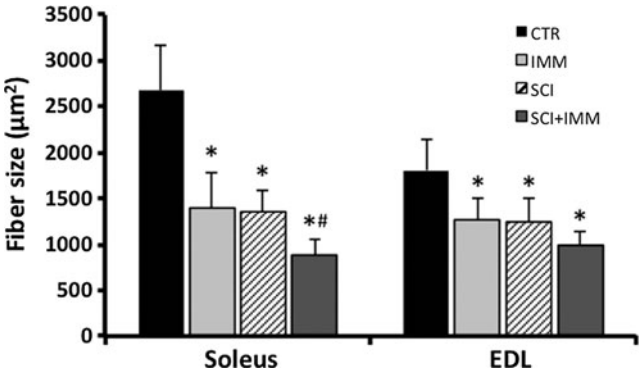

FIG. 5. Soleus and extensor digitorum longus (EDL) fiber cross-sectional area (μm^2). *Significantly different from controls (CTR). #Significantly different from spinal cord injured (SCI) ($p < 0.05$).

Discussion

The primary purpose of this study was to develop and validate a new rat model of severe SCI combined with cast immobilization, to better reproduce the condition observed in humans with SCI. Patients with SCI experience further muscle inactivity following injury, because of being on bed rest during the acute phase of recovery, and having limited mobility or using a wheelchair during the chronic phase. Overall, cast immobilization following contusion SCI in rats produced a greater loss in muscle size/mass and force production than SCI alone, and prevented spontaneous recovery. Our data suggest that SCI + IMM can be used to better identify the respective influences of the neural input and mechanical loading on skeletal muscle adaptations after SCI, providing a clinically relevant rodent model of SCI.

Spontaneous reversal of the muscle atrophy process after moderate contusion SCI has been previously observed by our group,[20] as well as in several other laboratories.[14,30] Recently, Caudle et al.[18] used hindlimb wheelchair immobilization (15–18 h/day and 5 days/week) to reduce the in-cage activity, which dramatically delayed spontaneous functional recovery after moderate SCI. Here, we extended this approach by restricting muscle activity for 24 h/day and 7 days/week. The model described here: 1) significantly reduced the reloading input; 2) was easily performed, with no evidence of infection at the surgical site or casted skin and no

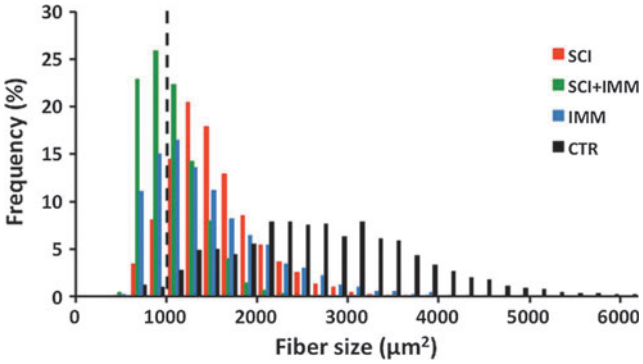

FIG. 6. Averaged muscle fiber size distributions in soleus muscle of control (CTR) spinal cord injured (SCI), immobilized (IMM), and both spinal cord injured and immobilized (SCI + IMM) animals. The dashed line represents the fifth percentile threshold for the CTR group.

Table 2. Degree of Asymmetry in the TS Muscles Size between Left and Right Limbs for All Groups

	Asymmetry coefficient (%)			
day	*CTR*	*IMM*	*SCI*	*SCI+IMM*
0	2.7±0.7	3.0±0.7	3.3±0.6	2.6±0.5
7	1.8±0.5	1.9±0.3	6.9±1.0*	4.7±0.8
14	2.4±0.7	4.3±1.2	11.8±2.4*#	11.7±2.6*#
21	3.0±0.5	4.4±1.2	9.6±2.4	14.9±3.4*#

*Significantly different from control values.
#Significantly different from baseline values.

significant loss in body weight compared with SCI alone; 3) maintained mortality rates of 29.5% in SCI and 38.5% in SCI+IMM, which was in the range of the values reported in the literature for moderate SCI (33.3%).[31] The present work proposes a reproducible experimental model of severe spinal contusion combined with bilateral limb cast immobilization.

Our model produced a dramatic drop of the BBB scores after 7 days, consistent with the values reported by Basso et al.[14] using the same injury protocol. One unique aspect of our study is that muscle size was characterized longitudinally, using noninvasive MRI. We demonstrated that CSA_{max} of the TS muscles was highly correlated to muscle wet weight measured at 21 days post-injury, regardless of the group. A maximum decline of 25% in TS CSA_{max} was reached after 1 week in SCI. This was similar to our previous observation[20] in a model of moderate SCI after 2 weeks, and was consistent with the changes in muscle mass reported by Hutchinson et al.[30] after moderate SCI. Although the amount of atrophy was similar between severe and moderate SCI after 1 week, several major differences were observed. First, our model induced significant atrophy in all of the tested muscles – including 10% decrease in EDL muscle wet weight after 3 weeks – whereas the EDL was not significantly affected in moderate SCI.[30] Second, the time course of muscle mass recovery was significantly slower after severe SCI. Muscle mass was still 27% lower in severe SCI compared with controls after 3 weeks in the soleus, a major postural muscle. This is in contrast with the value reported in moderate contusion SCI, in which soleus wet weight recovered within 3 weeks.[30] Overall, severe SCI produced the same maximal amount of atrophy as the moderate models, and showed a significant delay in spontaneous recovery.

Unlike human SCI patients, ambulation and movement are unrestricted in rats following experimental SCI once they are returned to the cage. This results in a considerable amount of mechanical loading.[14,20] To overcome this limitation, we applied bilateral cast immobilization in the SCI rats to reduce muscle loading. Muscle loading during locomotion has been shown to play an important role in shaping muscle activity after SCI.[32–34] For example, in humans with incomplete and complete SCI, partial lower limb loading significantly increased the amplitude of gastrocnemius EMG activity.[35] It has also been demonstrated that unloading one of the hindlimbs during treadmill training in de-cerebrated cats reduces the magnitude of ankle extensor EMG by 70%.[36] In addition, loading activity modulates the stepping and stance in locomotor control as the main source of afferent input to the spinal central pattern generator.[37,38] Our data showed that cast immobilization alone led to a similar or even larger percentage of loss in muscle mass and size in the posterior compartment muscles in comparison with severe SCI, which further demonstrates the importance of loading input in muscle plasticity. In the SCI+IMM group, the addition of cast immobilization minimized the loading on the muscle, allowing for examination of the role of neuromuscular activity and/or loading in the muscle adaptations after SCI. This model is more consistent with what is generally observed in human complete or chronic incomplete SCI,[39–42] in which patients usually experience an extended period of bed rest and reduced activity during the acute phase of the injury, up to several weeks. The primary muscles of ambulation continue to experience reduced loading for several weeks to months after SCI as activity-based rehabilitation is delayed by other post–traumatic complications.[32]

Whereas muscle peak tetanic force production was significantly reduced in all of the disuse conditions implemented in this study, the change in force was proportional to the extent of muscle atrophy. The normalized peak tetanic force of the soleus muscle among the different disuse models was similar to control values. From a functional perspective, this finding is of interest, as a greater loss of muscle mass induced by cast immobilization in the SCI model was not accompanied by loss in the normalized peak tetanic force or muscle quality. The degree of muscle atrophy from cast immobilization is also highly dependent on the length of the immobilized muscle.[43] Muscles immobilized in a shortened position experience a greater reduction in the normalized peak tetanic force.[44,45] In our study, muscles were immobilized in a neutral (resting) position and we did not observe a decrease in the normalized peak tetanic force, which is consistent with the literature.[44] Interestingly, we did not see a significant change in the normalized peak tetanic force of the soleus muscle in SCI+IMM either. It has been reported that normalized tetanic force in the muscle can increase,[46] decrease,[30] or be maintained[47,48] after SCI. A potential confounding factor in determining normalized peak tetanic force might be the inaccurate estimation of the contractile muscle mass or area. Muscle degeneration is often paralleled by an increase in intramuscular fat, and eventually by fibrosis as observed in aging[49] and clinical conditions such as muscular dystrophy.[50] In human chronic SCI, intramuscular fat infiltration and tissue scaring have been observed,[51] and correction for muscle fat content is necessary when measuring muscle size, in order to avoid inaccurate estimation.[52,53] Another reason for the discrepancies in the findings of normalized tetanic force may be the initial loss of slow rather than fast myofibril proteins in the early stages of muscle disuse.[54,55] Several studies suggested that fast-twitch muscle fibers generate a higher specific force than do slower fibers.[56,57] Assessment of myosin heavy chain composition may be warranted in future studies.

To further characterize this new model, we uniquely investigated the changes in muscle size across different disuse models in the soleus muscle, which is the primary loading muscle in the hindlimb in rodents. The present results showed that the fiber size distribution of soleus was identical in the SCI and casted rats. However, a greater shift towards smaller muscle fiber sizes was observed in the SCI+IMM group. It has been reported that SCI results in reduced average muscle fiber size after the injury. However, little is known about the degree of atrophy in the individual muscle fibers. The size distribution of muscle fibers has important implications for the quality of the muscle (cellularity), and is correlated with the body size.[58] The maximum force is proportional to the cross-sectional area of the individual muscle fibers. It is likely that the size distribution of fiber diameters will determine the time course for the progression of force production as well as the structural changes, such as amounts of collagen and cytoskeletal proteins per unit muscle volume.

An original observation of the present study is the changes in asymmetry between limb sizes over time. The levels of asymmetry measured in control animals were low and stable over time and might reflect the small variability in animal positioning in the magnet, in manual outlining of the muscles, as well as a natural asymmetry of the animals. It was interesting to observe that the cast immobilization affected both limbs in a symmetrical way. On the other hand, SCI led to an increased asymmetry within 7 days. This most likely reflects a slight asymmetry in the way the contusion was produced on the spinal cord. Surprisingly, the asymmetry in muscle size further increased at days 14 and 21, not only in SCI alone, but also in SCI + IMM, suggesting that despite the cast, the modulation in muscle size was still partially driven by the consequences of the injury. Whereas in SCI only the possibility of an asymmetric reloading pattern with free activity preferentially enhancing muscle size in one hindlimb cannot be excluded, SCI + IMM may offer a more unbiased model to specifically observe the neural aspect of muscle changes post-injury. In this case, the increased asymmetry in muscle size is likely to be related either to asymmetry in residual white matter pathways and subsequent ability to contract motor neuron and motor units, or to the progression of secondary injury mechanisms,[59] which have been documented to produce further damage up to several weeks post-injury.[60]

Changes in neural activation and/or limb loading contribute to skeletal muscle atrophy and hypertrophy, especially in the hindlimb muscles of rodents. Therefore, it is important to determine the differences and similarities across different models of muscle atrophy. From a rehabilitation standpoint, it is also essential to address the possible changes in muscle quality and function associated with SCI and cast immobilization. Our results show that SCI combined with cast immobilization adequately represents the disuse conditions inherent to the clinical condition of SCI. In human SCI, extended bed rest after injury further decreases muscle loading in addition to the reduced neural activation, which causes a greater degree of muscle atrophy to be reached before rehabilitation interventions are initiated. The new model of SCI-IMM implemented in this study will allow for an accurate assessment of the efficacy of therapeutic interventions and facilitate the translation to the clinical setting.

Acknowledgments

The authors thank James Colee for statistical analysis. This work was supported by grants from the National Institutes of Health (PO1 HD059751-01A1), the United States Department of Veterans Affairs (VA Rehabilitation R&D Merit Review B5037R), and the National High Magnetic Field Laboratory.

Author Disclosure Statement

No competing financial interests exist.

References

1. Biering-Sørensen, B., Kristensen, I.B., Kjaer, M., and Biering-Sørensen, F. (2009). Muscle after spinal cord injury. Muscle Nerve 40, 499–519.
2. Goodpaster, B.H., Thaete, F.L., and Kelley, D.E. (2000). Thigh adipose tissue distribution is associated with insulin resistance in obesity and in type 2 diabetes mellitus. Am. J. Clin. Nutr. 71, 885–892.
3. Aubertin–Leheudre, M., Lord, C., Goulet, É.D.B., Khalil, A., and Dionne, I.J. (2006). Effect of Sarcopenia on Cardiovascular Disease Risk Factors in Obese Postmenopausal Women. Obesity. 14, 2277–2283.
4. Barbagallo, M., and Dominguez, L.J. (2007). Magnesium metabolism in type 2 diabetes mellitus, metabolic syndrome and insulin resistance. Arch. Biochem. Biophys. 458, 40–47.
5. Crepaldi, G., and Maggi, S. (2005). Sarcopenia and osteoporosis, A hazardous duet. J. Endocrinol. Invest. 28, 66.
6. Buunk, A.P., Zurriaga, R., Gonzalez, P., Terol, C., and Roig, S.L. (2006). Targets and dimensions of social comparison among people with spinal cord injury and other health problems. Br. J. Health Psychol. 11, 677–693.
7. Crozier, K., Cheng, L.L., Graziani, V., Zorn, G., Herbison, G., and Ditunno, J. (1992). Spinal cord injury: prognosis for ambulation based on quadriceps recovery. Spinal Cord 30, 762–767.
8. Frost, F. (1993). Role of rehabilitation after spinal cord injury. Urol. Clin. N. Am. 20, 549.
9. Onifer, S.M., Rabchevsky, A.G., and Scheff, S.W. (2007). Rat models of traumatic spinal cord injury to assess motor recovery. ILAR J. 48, 385–95.
10. Wrathall, J. (1992). Spinal cord injury models. J. Neurotrauma 9, S129.
11. Young, W. (2002). Spinal cord contusion models. Progr. Brain Res. 137, 231–255.
12. Bunge, R., Puckett, W., Becerra, J., Marcillo, A., and Quencer, R. (1993). Observations on the pathology of human spinal cord injury. A review and classification of 22 new cases with details from a case of chronic cord compression with extensive focal demyelination. Adv. Neurol. 59, 75.
13. Basso, D.M., Beattie, M.S., and Bresnahan, J.C. (1995). A sensitive and reliable locomotor rating scale for open field testing in rats. J. Neurotrauma 12, 1–21.
14. Basso, D.M., Beattie, M.S., and Bresnahan, J.C. (1996). Graded histological and locomotor outcomes after spinal cord contusion using the NYU weight-drop device versus transection. Exp. Neurol. 139, 244–256.
15. Gruner, J.A. (1992). A monitored contusion model of spinal cord injury in the rat. J. Neurotrauma 9, 123–128.
16. Stevens, J.E., Liu, M., Bose, P., O'Steen, W.A., Thompson, F.J., Anderson, D.K., and Vandenborne, K. (2006). Changes in soleus muscle function and fiber morphology with one week of locomotor training in spinal cord contusion injured rats. J. Neurotrauma 23, 1671–1681.
17. Young, W., Kume-Kick, J., and Constantini, S. (1994). Glucocorticoid therapy of spinal cord injury. Ann. N. Y. Acad. Sci. 743, 241–263.
18. Caudle, K.L., Brown, E.H., Shum–Siu, A., Burke, D.A., Magnuson, T.S.G., Voor, M.J., and Magnuson, D.S.K. (2011). Hindlimb immobilization in a wheelchair alters functional recovery following contusive spinal cord injury in the adult rat. Neurorehabil. Neural Repair 25, 729–739.
19. Fouad, K., Metz, G.A.S., Merkler, D., Dietz, V., and Schwab, M.E. (2000). Treadmill training in incomplete spinal cord injured rats. Behav. Brain Res. 115, 107–113.
20. Liu, M., Bose, P., Walter, G.A., Thompson, F.J., and Vandenborne, K. (2008). A longitudinal study of skeletal muscle following spinal cord injury and locomotor training. Spinal Cord 46, 488–493.
21. Singh, A., Balasubramanian, S., Murray, M., Lemay, M., and Houle, J. (2011). Role of spared pathways in locomotor recovery after body-weight-supported treadmill training in contused rats. J. Neurotrauma 28, 2405–2401.
22. Smith, R.R., Shum–Siu, A., Baltzley, R., Bunger, M., Baldini, A., Burke, D.A., and Magnuson, D.S.K. (2006). Effects of swimming on functional recovery after incomplete spinal cord injury in rats. J. Neurotrauma 23, 908–919.
23. Stevens, L., Bastide, B., Kischel, P., Pette, D., and Mounier, Y. (2002). Time-dependent changes in expression of troponin subunit isoforms in unloaded rat soleus muscle. Am. J. Physiol. Cell Physiol. 282, 1025–1030.
24. van Meeteren, N.L.U., Eggers, R., Lankhorst, A.J., Gispen, W.H., and Hamers, F.P.T. (2003). Locomotor recovery after spinal cord contusion injury in rats is improved by spontaneous exercise. J. Neurotrauma 20, 1029–1037.
25. Booth, F.W., and Kelso, J.R. (1973). Production of rat muscle atrophy by cast fixation. J. Appl. Physiol. 34, 404–406.
26. Frimel, T.N., Kapadia, F., Gaidosh, G.S., Li, Y., Walter, G.A., and Vandenborne, K. (2005). A model of muscle atrophy using cast immobilization in mice. Muscle Nerve 32, 672–674.

27. Pathare, N., Vandenborne, K., Liu, M., Stevens, J.E., Li, Y., Frimel, T.N., and Walter, G.A. (2008). Alterations in inorganic phosphate in mouse hindlimb muscles during limb disuse. NMR Biomed. 21, 101–110.
28. Thompson, F., Reier, P., Lucas, C., and Parmer, R. (1992). Lumbar spinal reflex excitability following contusion injury of the mid-thoracic spinal cord. J. Neurophysiol. 68, 1473–1486.
29. Stevens, J.E., Liu, M., Bose, P., O'Steen, W.A., Thompson, F.J., Anderson, D.K., and Vandenborne, K. (2006). Changes in soleus muscle function and fiber morphology with one week of locomotor training in spinal cord contusion injured rats. J. Neurotrauma 23, 1671–1681.
30. Hutchinson, K.J., Linderman, J.K., and Basso, D.M. (2001). Skeletal muscle adaptations following spinal cord contusion injury in rat and the relationship to locomotor function: a time course study. J. Neurotrauma 18, 1075–1089.
31. Wrathall, J.R., Pettegrew, R.K., and Harvey, F. (1985). Spinal cord contusion in the rat: production of graded, reproducible, injury groups. Exp. Neurol. 88, 108–122.
32. Behrman, A.L., Bowden, M.G., and Nair, P.M. (2006). Neuroplasticity after spinal cord injury and training: an emerging paradigm shift in rehabilitation and walking recovery. Phys. Ther. 86, 1406–1425.
33. Frigon, A., and Rossignol, S. (2006). Functional plasticity following spinal cord lesions. Prog. Brain Res. 157, 231–398.
34. Pearson, K. (2008). Role of sensory feedback in the control of stance duration in walking cats. Brain Res. Rev. 57, 222–227.
35. Dietz, V., and Duysens, J. (2000). Significance of load receptor input during locomotion: a review. Gait Posture 11, 102–110.
36. Gerasimenko, Y.P., Avelev, V., Nikitin, O., and Lavrov, I. (2003). Initiation of locomotor activity in spinal cats by epidural stimulation of the spinal cord. Neurosci. Behav. Physiol. 33, 247–254.
37. Dimitrijevic, M.R., Gerasimenko, Y., and Pinter, M.M. (1998). Evidence for a spinal central pattern generator in humans. Ann. N. Y. Acad. Sci. 860, 360–376.
38. Rossignol, S. (1996). Neural control of stereotypic limb movements, in: *Handbook of Physiology, Section 12. Exercise: Regulation and Integration of Multiple Systems, Volume 12, Chapter 5.* Rowell, L.B., and Sheperd, J.T. (eds). American Physiological Society: Oxford, pps. 173–216.
39. Adams, M.M., Ditor, D.S., Tarnopolsky, M.A., Phillips, S.M., McCartney, N., and Hicks, A.L. (2006). The effect of body weight-supported treadmill training on muscle morphology in an individual with chronic, motor-complete spinal cord injury: A case study. J. Spinal Cord Med. 29, 167–171.
40. Castro, M.J., Apple, D.F., Jr., Staron, R.S., Campos, G.E.R., and Dudley, G.A. (1999). Influence of complete spinal cord injury on skeletal muscle within 6 mo of injury. J. Appl. Physiol. 86, 350–358.
41. Gregory, C.M., Vandenborne, K., Castro, M.J., and Dudley, G.A. (2003). Human and rat skeletal muscle adaptations to spinal cord injury. Can. J. Appl. Physiol. 28, 491–500.
42. Shah, P.K., Gregory, C.M., Stevens, J.E., Pathare, N.C., Jayaraman, A., Behrman, A.L., Walter, G.A., and Vandenborne, K. (2008). Non-invasive assessment of lower extremity muscle composition after incomplete spinal cord injury. Spinal Cord 46, 565–570.
43. Hnik, P., Vejsada, R., Goldspink, D.F., Kasicki, S., and Krekule, I. (1985). Quantitative evaluation of electromyogram activity in rat extensor and flexor muscles immobilized at different lengths. Exp. Neurol. 88, 515–528.
44. Simard, C., Spector, S., and Edgerton, V. (1982). Contractile properties of rat hind limb muscles immobilized at different lengths. Exp. Neurol. 77, 467–482.
45. Stevens–Lapsley, J.E., Ye, F., Liu, M., Borst, S.E., Conover, C., Yarasheski, K.E., Walter, G.A., Sweeney, H.L., and Vandenborne, K. (2010). Impact of viral-mediated IGF-I gene transfer on skeletal muscle following cast immobilization. Am. J. Physiol. Endocrinol. Metab. 299, E730–740.
46. Lieber, R.L., Johansson, C.B., Vahlsing, H.L., Hargens, A.R., and Feringa, E.R. (1986). Long-term effects of spinal cord transection on fast and slow rat skeletal muscle. I. Contractile properties. Exp. Neurol. 91, 423–434.
47. Landry, E., Frenette, J., and Guertin, P.A. (2004). Body weight, limb size, and muscular properties of early paraplegic mice. J. Neurotrauma 21, 1008–1016.
48. Talmadge, R.J., Roy, R.R., Caiozzo, V.J., and Edgerton, V.R. (2002). Mechanical properties of rat soleus after long-term spinal cord transection. J. Appl. Physiol. 93, 1487–1497.
49. Larsson, L., and Edström, L. (1986). Effects of age on enzyme-histochemical fibre spectra and contractile properties of fast-and slow-twitch skeletal muscles in the rat. J. Neurol. Sci. 76, 69–89.
50. Deconinck, N., and Dan, B. (2007). Pathophysiology of duchenne muscular dystrophy: current hypotheses. Pediatr. Neurol. 36, 1–7.
51. Elder, C., Apple, D., Bickel, C., Meyer, R., and Dudley, G. (2004). Intramuscular fat and glucose tolerance after spinal cord injury–a cross-sectional study. Spinal Cord 42, 711–716.
52. Gorgey, A., and Dudley, G. (2006). Skeletal muscle atrophy and increased intramuscular fat after incomplete spinal cord injury. Spinal Cord 45, 304–309.
53. Gorgey, A., and Dudley, G. (2007). Spasticity may defend skeletal muscle size and composition after incomplete spinal cord injury. Spinal Cord 46, 96–102.
54. Salmons, S., and Sreter, F. (1976). Significance of impulse activity in the transformation of skeletal muscle type. Nature 263, 30–34
55. Thomason, D., Herrick, R., Surdyka, D., and Baldwin, K. (1987). Time course of soleus muscle myosin expression during hindlimb suspension and recovery. J. Appl. Physiol. 63, 130–137.
56. Harridge, S.D.R., Bottinelli, R., Canepari, M., Pellegrino, M., Reggiani, C., Esbjörnsson, M., and Saltin, B. (1996). Whole-muscle and single-fibre contractile properties and myosin heavy chain isoforms in humans. Pflügers Arch. 432, 913–920.
57. Rome, L.C., Sosnicki, A.A., and Goble, D. (1990). Maximum velocity of shortening of three fibre types from horse soleus muscle: implications for scaling with body size. J. Physiol. 431, 173–185.
58. Weatherley, A., Gill, H., and Rogers, S. (1979). Growth dynamics of muscle fibres, dry weight, and condition in relation to somatic growth rate in yearling rainbow trout (Salmo gairdneri). Can. J. Zool. 57, 2385–2392.
59. Oyinbo, C.A. (2011). Secondary injury mechanisms in traumatic spinal cord injury: a nugget of this multiply cascade. Acta. Neurobiol. Exp. (Wars.) 71, 281–299.
60. Tanhoffer, R.A., Yamazaki, R.K., Nunes, E.A., Pchevozniki, A.I., Pchevozniki, A.M., Nogata, C., Aikawa, J., Bonatto, S.J., Brito, G., and Lissa, M.D. (2007). Glutamine concentration and immune response of spinal cord–injured rats. J. Spinal Cord Med. 30, 140–146.

Address correspondence to:
Celine Baligand, PhD
Department of Physiology and Functional Genomic
University of Florida
PO Box 100274
Gainesville, FL 32610

E-mail: baligand@ufl.edu